MICROCOPY RESOLUTION TEST CHART
NATIONAL BUREAU OF STANDARDS-1963-A

RADC-TR-85-152
Final Technical Report
August 1985

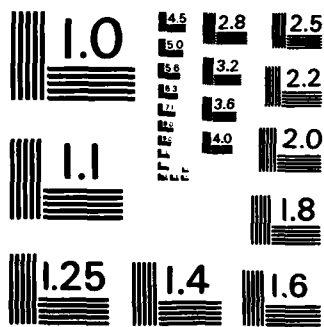# OBSERVATIONS OF SUB-LF ELECTROMAGNETIC FIELD PHENOMENA ASSOCIATED WITH MODULATED ELECTRON BEAMS ON STS-3

AD-A162 543

Stanford University

Antony C. Fraser-Smith
Peter M. Banks
Geoffery D. Reeves

DTIC
ELECTE
DEC 20 1985
S   D
             B

ROME AIR DEVELOPMENT CENTER
Air Force Systems Command
Griffiss Air Force Base, NY 13441-5700

DTIC FILE COPY

85 12 20 004

This report has been reviewed by the RADC Public Affairs Office (PA) and is releasable to the National Technical Information Service (NTIS). At NTIS it will be releasable to the general public, including foreign nations.

RADC-TR-85-152 has been reviewed and is approved for publication.
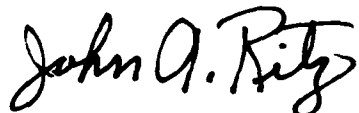
APPROVED: *[signature]*

DALLAS T. HAYES
Project Engineer

APPROVED: *[signature]*

ALLAN C. SCHELL
Chief, Electromagnetic Sciences Division

FOR THE COMMANDER: *[signature]*

JOHN A. RITZ
Acting Chief, Plans Office

-D, A/c-2543

REPORT DOCUMENTATION PAGE

1a REPORT SECURITY CLASSIFICATION	1b RESTRICTIVE MARKINGS
UNCLASSIFIED	N/A

2a SECURITY CLASSIFICATION AUTHORITY	3 DISTRIBUTION/AVAILABILITY OF REPORT
N/A	Approved for public release;
2b DECLASSIFICATION/DOWNGRADING SCHEDULE	distribution unlimited.
N/A	

4 PERFORMING ORGANIZATION REPORT NUMBER(S)	5 MONITORING ORGANIZATION REPORT NUMBER(S)
N/A	RADC-TR-85-152

6a NAME OF PERFORMING ORGANIZATION	6b OFFICE SYMBOL (If applicable)	7a NAME OF MONITORING ORGANIZATION
Stanford University		NASA Headquarters

6c. ADDRESS (City, State, and ZIP Code)	7b ADDRESS (City, State, and ZIP Code)
Space, Telecommunications & Radioscience Laboratory Stanford CA 94035	Code EE8 Wash DC 20546

8a NAME OF FUNDING/SPONSORING ORGANIZATION	8b OFFICE SYMBOL (If applicable)	9 PROCUREMENT INSTRUMENT IDENTIFICATION NUMBER
Rome Air Development Center	EEP	NASA Grant NAGW-235

8c ADDRESS (City, State, and ZIP Code)	10 SOURCE OF FUNDING NUMBERS			
Hanscom AFB MA 01731	PROGRAM ELEMENT NO	PROJECT NO	TASK NO	WORK UNIT ACCESSION NO
	61101F	2305	J2	45

11 TITLE (Include Security Classification)
OBSERVATIONS OF SUB-LF ELECTROMAGNETIC FIELD PHENOMENA
ASSOCIATED WITH MODULATED ELECTRON BEAMS ON STS-3

12 PERSONAL AUTHOR(S)
Antony C. Fraser-Smith, Peter M. Banks, Geoffery D. Reeves

13a TYPE OF REPORT	13b TIME COVERED	14 DATE OF REPORT (Year, Month, Day)	15 PAGE COUNT
Final	FROM Apr 83 TO Mar 84	August 1985	44

16 SUPPLEMENTARY NOTATION
N/A

17 COSATI CODES			18 SUBJECT TERMS (Continue on reverse if necessary and identify by block number)
FIELD	GROUP	SUB-GROUP	Electron Beam > Space Plasma
04	01		Space Shuttle Beam Plasma Interactions
17	02		ULF, ELF, VLF

19 ABSTRACT (Continue on reverse if necessary and identify by block number)

In this report we provide initial documentation of some of the sub-LF (frequencies less than 30kHz) electromagnetic field phenomena observed during the first active electron-beam/space plasma experiment on a Space Shuttle orbiter. The experiment took place in March 1982 as part of the NASA Office of Space Science mission on the third flight of an orbiter, and it was notable for its particularly complete instrumentation for plasma and electromagnetic wave diagnostic measurements. A number of anomalous electric and magnetic field phenomena are observed during the electron beam modulation experiments, including the generation of noise bands, extra harmonics, and a variety of side frequencies. In addition, discrete ELF tones are observed during some of the dc electron beam pulse sequences, and there are peculiarities in the harmonic structure of the electromagnetic fields produced during lower-ELF modulation of the electron beam. Studies of these effects are continuing.

20 DISTRIBUTION/AVAILABILITY OF ABSTRACT	21 ABSTRACT SECURITY CLASSIFICATION
[X] UNCLASSIFIED/UNLIMITED ☐ SAME AS RPT ☐ DTIC USERS	UNCLASSIFIED

22a NAME OF RESPONSIBLE INDIVIDUAL	22b TELEPHONE (Include Area Code)	22c OFFICE SYMBOL
DALLAS T. HAYES	(617) 861-4265	RADC (EEP)

DD FORM 1473, 84 MAR   83 APR edition may be used until exhausted   SECURITY CLASSIFICATION OF THIS PAGE
All other editions are obsolete

UNCLASSIFIED

Block 17 (Cont'd)

Field   Group
20   14

ACKNOWLEDGEMENTS

DTIC
ELECTE
DEC 20 1985
S D
B

QUALITY
INSPECTED
3

A-1

TABLE OF CONTENTS

A NOTE ON FREQUENCIES

In this report we use the abbreviation ULF (ultra-low frequencies) for frequencies less than 5 Hz. Pc 1 geomagnetic pulsations are observed in the upper part of this frequency range (0.2 - 5 Hz). ELF (extremely-low frequencies) is used to designate frequencies in the range 5 Hz to 3 kHz. For frequencies ranges above the ELF range the abbreviations are conventional: VLF (very-low frequencies) is used for frequencies in the range 3 - 30 kHz, and LF (low frequencies) for frequencies in the range 30 - 300 kHz.

1. INTRODUCTION

A wide range of experiments with electron beams have been carried out in space and in space simulation chambers to investigate a variety of different phenomena, including: (1) the radiating characteristics of an electron beam [*e.g., Cartwright and Kellogg*, 1974], (2) one or another of a variety of beam-plasma interactions [*e.g., Cartwright and Kellogg*, 1971], (3) the generation of artificial aurora [*e.g., Hess*, 1969], and (4) the diagnostic capabilities of the electron beams, *i.e.*, their ability to delineate geomagnetic field lines, to measure electric fields in the magnetosphere, or, generally, to probe the magnetosphere [*e.g., Hendrickson et al.*, 1971; *Cambou et al.*, 1978]. The literature describing these experiments, covering the relevant theory, and comparing the experimental results with theory is extensive [see reviews by *Linson and Papadopoulos*, 1980; *Winckler*, 1980; *Grandal*, 1982], and its volume provides a good indication of the rapid developments in the 16 years since the first electron beam experiment in space [*Hess*, 1969]. However, these early experiments were limited by the fact that, with the exception of a few satellite experiments [*e.g., Meltzner et al.*, 1978], the electron beams had to be injected into the ionosphere and magnetosphere with research rockets, meaning that there was little time available for the experiments. This situation has now changed, due to the availability of the Space Shuttle orbiters as platforms for electron beam experiments in space. An electron gun was flown on an orbiter for the first time during the March 22 - 30, 1982, flight of the *Columbia*, and electron beam experiments were carried out for a total of many hours of beam time. There have since been two other electron beam experiments on an orbiter (the SEPAC and PICPAB experiments on Spacelab-1, which took place in December, 1983), and one more is planned for 1985. The large amount of time that can be devoted to electron beam experiments on these missions, under greatly varying ionospheric, magnetospheric, and ambient plasma conditions, should ensure rapid progress in our understanding of how the beams propagate in space plasmas.

The purpose of this report is to document some of the low-frequency electromagnetic field phenomena observed during the first electron beam experiment on the shuttle *Columbia*. Since the third flight of a shuttle was involved, it is frequently referred to as STS-3, where the letters stand for Space Transportation System. Further, because the scientific payload was originally managed by the Office of Space Science at NASA

headquarters, the scientific payload on STS-3 is often given the designation OSS-1. Thus we may refer to the OSS-1 instrument packages, or experiments, on STS-3. All but one of the OSS-1 instrument packages were mounted on a pallet manufactured by the European Space Agency and located in the payload bay. The electron beam generator was part of one of the nine OSS-1 instrument packages; it is referred to as the Fast Pulse Electron Generator, or FPEG. The FPEG was an integral part of the Vehicle Charging and Potential (VCAP) experiment, the purpose of which was to make vehicle charging and electron beam studies - the first on a manned spacecraft. In addition to the FPEG, the VCAP package included two pairs of charge and current probes, situated on opposite sides of the pallet, and ı Langmuir probe/spherical retarding potential analyzer mounted on the sill of the pallet. *Banks et al.* [1985] provide an extensive discussion of the VCAP instrumentation. The other OSS-1 package of relevance to the topic of this report is the Plasma Diagnostics Package, or PDP. As is indicated by its name, the primary purpose of the PDP was to measure the electromagnetic and plasma environment of the shuttle: through the use of various sensors, measurements were made of electric and magnetic fields, plasma waves, energetic ions and electrons, and plasma parameters such as density, composition, temperature, and directed velocity. A summary of the various PDP sensors and their measurement ranges is given in the Appendix; the reader is also referred to the papers by *Neupert et al.* [1982], *Shawhan and Murphy* [1983], and *Shawhan et al.* [1984a,b,c] for further technical details of the PDP. Another purpose of the PDP was to test the capabilities of the Remote Manipulator System (RMS) and to assist in the active electron beam-plasma experiments initiated with the FPEG. As it turned out, the PDP measurements provided an extraordinarily rich and detailed description of the electromagnetic and plasma changes in the vicinity of STS-3 during operations of the FPEG, and the measurements documented in this report are largely those of the electric and magnetic sensors on the PDP.

Turning now to some of the specific details of the electron beam experiments, the following are pertinent details of the FPEG:

- Beam energy: 1 keV.
- Beam current: 100 mA/50 mA.
- Beam power: 100 W/50 W.
- Beam current rise time: 100 ns.
- Beam divergence (on leaving FPEG): 7.5°.
- Minimum pulse length: 600 ns.

- Maximum pulse length: 107 s.

- Maximum pulse count: 32,768.

- Beam direction: vertical from the pallet.

Although the beam current is listed as having two possible levels, the 100 mA (largest) current was used for most of the STS-3 experiments. The applicable beam power for this current is 100 W. Figure 1 shows the location of the FPEG on the pallet, and in relation to the PDP. As noted above, the electron beam is directed vertically upwards from the pallet as it leaves the aperture of the gun, but it is immediately subject to forces due to the presence of the geomagnetic field and becomes deflected more or less from this initial reference direction depending on the strength and direction of the geomagnetic field. In general, unless it is initially deflected in such a manner to strike some surface of the shuttle, the beam travels away from the shuttle in a helix whose axis is directed along the geomagnetic field.

The STS-3 orbit was circular, with an inclination of $38.42°$, an altitude of 240 km, and an orbital period of 1 hr 29 min. These orbit parameters have a number of implications for the interpretation of the results of the electron beam experiments. First, the shuttle was located in the F region of the ionosphere, or, more strictly, in the F_2 region, close to the electron density peak. It would be expected that the ambient electron density would lie in the range 10^5 - 10^7 cm^{-3}, with the smaller values occurring at night, and the atmospheric pressure should be close to 4.3×10^{-7} torr, or about 6×10^{-10} atm. The predominant ion should be O^+. Second, because of the inclination of its orbit, the shuttle's measurements were always made at low or equatorial latitudes. Third, the orbital speed of the shuttle was close to 7.8 km/s, which is very much greater than the ion or neutral gas speed of sound at that altitude. Because of its supersonic speed, the shuttle was surrounded by a wake and preceded by a bow shock. When the payload bay was facing forward the atmospheric gases and plasma were 'rammed' into the bay, whereas when the bay was facing away from the direction of motion, *i.e.*, facing in the wake direction, the shuttle blocked the flow into the bay and it was difficult for the atmospheric gases and plasma to enter. The plasma conditions in the bay therefore varied greatly between what are conventionally referred to as *ram* and *wake* conditions.

STS-3 was launched at 1600 UT on March 22, 1982, corresponding to day 81 of the year 1983. It landed at 1613 UT on March 30, 1982 (day 89), with its descent beginning from the 129th orbit. The first regular sequence of electron beam firings began at 1720

3

UT on March 23 (day 82) and terminated at 0200 UT on March 29 (day 88). The beam could be square-wave modulated with frequencies varying from essentially zero (dc pulses) up to the megahertz range. However, a full range of PDP measurements could only be made for frequencies in the range 0 - 30 kHz. Partly for this reason, but more particularly because our interest in this report is in the potential use of modulated electron beams in space as 'wireless' antennas for the generation of low-frequency signals for communication, we restrict our discussion to electromagnetic field measurements at frequencies less than 30 kHz; i.e., to frequencies in the sub-LF range.

In the following section we describe the electron beam experiments that were conducted at frequencies in this sub-LF range. Then, in the following section, we document some of the interesting sub-LF phenomena that were observed.

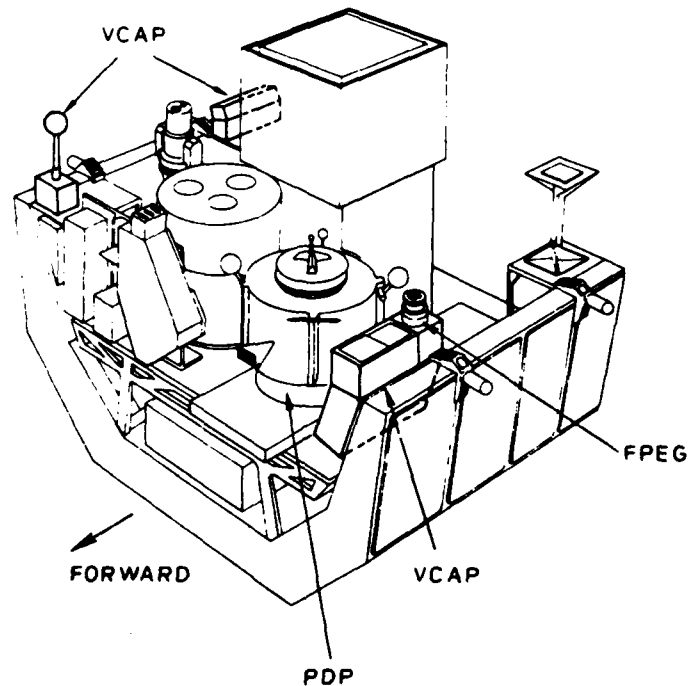**Figure 1:** Sketch of the OSS-1 instrumentation mounted on its pallet. The two parts of the vehicle charging and potential (VCAP) instrumentation are shown, and the fast pulse electron gun (FPEG) can be seen on the port side of the pallet, directed vertically upward from the pallet. Photographs of this pallet in place in the payload bay of *Columbia* can be seen in the article by *Shawhan et al.* [1984a].

5

2. THE STS-3 SUB-LF ELECTRON BEAM EXPERIMENTS

The sub-LF experiments of interest can be conveniently divided into three different categories:

1. DC beams.
2. ULF/ELF beam modulation.
3. VLF beam modulation.

As we shall now describe, there was a clear distinction in frequency between experiments in these three different categories.

2.1 DC Beams

In these experiments the electron beam modulation was very simple: the FPEG was turned on for some tens of seconds and then turned off. The most intensive of these experiments took place on March 25 (day 84), where, from 0116 - 0143 UT, during orbital darkness, the electron beam was emitted from the FPEG in a series of 53.69-second dc pulses. The time interval between the starting times of these pulses was roughly two minutes, and a total of 13 pulses were produced. In addition to this particular experiment, it was common for two 53.69-second dc pulses spaced 13.42 s apart to be generated at the end of the CC sequences to be described in the following section.

2.2 ULF/ELF Beam Modulations

Two ULF/ELF modulation sequences were used extensively throughout the STS-3 mission. These sequences will be referred to as CC (Charge and Coupling) and WS (Wave Stimulation) sequences. Taking these sequences in turn, the CC sequence consisted of 12 sets of 16 pulses of the electron beam, with a short interval of 2 - 3 seconds duration separating each set from the adjacent sets during which the electron beam was turned off. The spacing between the pulses was maintained at 209.72 ms throughout, but the length of the pulses (the beam 'on' time) was increased in each succeeding set, varying from 400 ns in the first set to 209.72 ms in the last set. In the latter case the beam on and off times were equal. The following listing shows the various on times that were used and the pulse repetition frequencies:

• Details of CC Sequence

1. 16 pulses, on time = 400 ns, $f = 4.78$ Hz.
2. 16 pulses, on time = 1.0 μs, $f = 4.78$ Hz.
3. 16 pulses, on time = 3.4 μs, $f = 4.78$ Hz.
4. 16 pulses, on time = 13.0 μs, $f = 4.78$ Hz.
5. 16 pulses, on time = 51.4 μs, $f = 4.78$ Hz.
6. 16 pulses, on time = 205 μs, $f = 4.78$ Hz.
7. 16 pulses, on time = 819 μs, $f = 4.77$ Hz.
8. 16 pulses, on time = 3.28 ms, $f = 4.71$ Hz.
9. 16 pulses, on time = 13.1 ms, $f = 4.50$ Hz.
10. 16 pulses, on time = 52.4 ms, $f = 3.83$ Hz.
11. 16 pulses, on time = 104.9 ms, $f = 3.19$ Hz.
12. 16 pulses, on time = 209.7 ms, $f = 2.39$ Hz.

As can be seen, there is not much difference between the highest and lowest pulse repetition frequencies in a CC sequence. However, there is a very substantial difference between the pulse on-times, which has significance from the point of view of the possible excitation of a beam plasma discharge (BPD) by the modulated electron beam.

The WS sequence covered the frequency range 2.31 - 74.0 Hz with 17 different sets of electron beam modulation patterns. Some higher frequencies were included in the complete sequence implemented on the shuttle, but the electron beam was only modulated for a short time (less than 0.3 s) at these frequencies and the frequencies all lay above the LF range and were thus largely above the frequency range for quantitative measurements by the PDP. We will only consider the WS sequence results at ULF/ELF frequencies. The following listing shows the various beam on and off times that were used and the pulse repetition frequencies:

• Details of WS Sequence

1. 512 pulses, on time = 13.11 ms, off time = 409.8 μs, $f = 73.97$ Hz.
2. 512 pulses, on time = 13.11 ms, off time = 1.64 ms, $f = 67.80$ Hz.
3. 512 pulses, on time = 13.11 ms, off time = 3.28 ms, $f = 61.01$ Hz.
4. 512 pulses, on time = 13.11 ms, off time = 6.55 ms, $f = 50.86$ Hz.
5. 256 pulses, on time = 13.11 ms, off time = 13.11 ms, $f = 38.14$ Hz.
6. 256 pulses, on time = 26.21 ms, off time = 3.28 ms, $f = 33.91$ Hz.
7. 256 pulses, on time = 26.21 ms, off time = 6.55 ms, $f = 30.53$ Hz.

8. 256 pulses, on time = 13.11 ms, off time = 26.21 ms, f = 25.43 Hz.

9. 128 pulses, on time = 26.21 ms, off time = 26.21 ms, f = 19.08 Hz.

10. 128 pulses, on time = 26.21 ms, off time = 52.43 ms, f = 12.72 Hz.

11. 64 pulses, on time = 52.43 ms, off time = 52.43 ms, f = 9.537 Hz.

12. 64 pulses, on time = 13.11 ms, off time = 104.86 ms, f = 8.477 Hz.

13. 64 pulses, on time = 26.21 ms, off time = 104.86 ms, f = 7.630 Hz.

14. 64 pulses, on time = 52.43 ms, off time = 104.86 ms, f = 6.358 Hz.

15. 32 pulses, on time = 13.11 ms, off time = 209.72 ms, f = 4.488 Hz.

16. 32 pulses, on time = 52.43 ms, off time = 209.72 ms, f = 3.815 Hz.

17. 16 pulses, on time = 13.11 ms, off time = 419.43 ms, f = 2.312 Hz.

It will be noted that all of the frequencies in the above two ULF/ELF sequences are less than 100 Hz. Interestingly, none of the regularly scheduled electron beam modulation experiments explored the frequency range 100 - 3,000 Hz, which is by far the largest part of the ELF range. Unlike the frequency range covered by the WS sequence detailed above, which includes a number of the ion gyrofrequencies that would be encountered at 240 km altitude, there is no particular reason to anticipate unusual beam/plasma interactions for beam modulation frequencies in the 100 - 3,000 Hz range. Nevertheless, in retrospect, it would have been desirable, if only from the point of view of completeness, for some of the beam experiments to have been conducted at selected frequencies throughout the entire ELF range. This omission will be corrected during experiments planned for the Spacelab-2 mission in July, 1985.

2.3 VLF Beam Modulations

Two VLF beam modulation sequences were used extensively during the STS-3 mission. Of these, the most frequently used sequence (usually designated the VLF1 sequence) involved a repetition of the two modulation frequencies 3.251 kHz and 4.473 kHz. The other sequence (VLF2), which will not be discussed further in this report, involved a repetition of the two modulation frequencies 19.38 kHz and 25.77 kHz. The following are the beam on and off times, and the number of pulses, for the VLF1 sequence:

● Details of VLF1 Sequence

1. 32,768 pulses, on time = 205.00 μs, off time = 102.60 μs, f = 3.251 kHz.

2. 32,768 pulses, on time = 102.60 μs, off time = 102.60 μs, f = 4.873 kHz.

The complete VLF1 sequence consisted of four repetitions of the above two sets of beam modulations. As a simple computation from the above data will verify, the

9

interval of modulation at 3.251 kHz lasted for about 10.1 s and the interval at 4.873 kHz lasted for about 6.7 s. During the experiments there was usually, but not always, an interval of about 12 s between the start of one of the intervals of beam modulation and the start of the next interval. Thus, there was a gap of about 2 s between the termination of an interval of modulation at 3.251 kHz and the start of an interval of modulation at 4.873 kHz; the corresponding gap between the 4.873 kHz and 3.251 kHz intervals was about 5 s. It will be noticed that a square wave modulation is used at 4.873 kHz, whereas at 3.251 kHz the on time of the pulses is close to twice the off time. This latter detail of the modulation patterns has significance for the generation of harmonics.

Once again we should note a gap in the modulation frequencies that were used: there were no modulations in the range 5 - 19 kHz. In future experiments it is planned to have some frequencies in this range, which is widely used by ground-based VLF transmitters.

3. RESULTS OF SUB-LF MEASUREMENTS

The results we present in this report are largely high-resolution dynamic spectrograms of PDP electric and magnetic field data recorded on a wide-band receiver. These data have a complex format that we will now describe, before presenting any of the data.

3.1 Data Format

As pointed out by *Shawhan et al.* [1984a], most of the measurements made by the PDP were limited in their time and frequency resolution by the time required to sample the outputs from the many different sensors. There were a total of 15 measurements that had to be made, and the sampling period was 0.1 sec, which meant that the time interval between successive samples of one particular measurement was 1.6 sec. As a result, effects occurring on time scales of less than a second could not be resolved. This limitation did not apply in the case of the data that were recorded continuously by the wide-band receiver (although, as we will now describe, there are certain necessary limitations in the data coverage due to the format that was adopted), and measurements using these latter data have high time and frequency resolution. In the VLF range, for example, the wide-band data have a time resolution of about 40 ms and a frequency resolution of 20 Hz [*Shawhan et al.*, 1984a].

The wide-band receiver was connected through a switching system to the AC electric field wave analyzer (electric antenna), to the search coil (magnetic antenna), and to the Langmuir probe (alternate electric antenna) on the PDP. Only the output from one antenna at a time could be recorded, so the switching system connected the receiver to one or the other of the three antennas according to the following scheme:

--Electric--Magnetic--Electric--Magnetic--Electric--Magnetic--Electric--LP--

where LP stands for Langmuir probe. This basic pattern of eight alternating intervals of electric and magnetic antenna measurements, with a Langmuir probe measurement substituted for every fourth of the magnetic measurements, was repeated continuously, with each interval lasting for 51.2 s.

In addition to the switching of antennas, there was also a pattern of switching in frequency. The nominal frequency range for the wide-band recordings was 5 Hz to 30

i⁹

kHz, but not all this range could be recorded at once. A basic frequency range of from ~400 Hz to about 15 kHz was available, and this was divided into two ranges: ~400 Hz to 10 kHz, and 13.5 ± 1 kHz. The former of these ranges was used for the general-purpose wide-band recordings and the latter for recording the ELF range ~5 Hz to 1 kHz. In order to fit the wide-band recordings into the available ~400 Hz to 10 kHz range they were broken into three segments of, nominally, 0 - 10 kHz, 10 - 20 kHz, and 20 - 30 kHz, and the two higher frequency ranges translated down in frequency to fit into the available range. During the translation process, the 10 - 20 kHz range was inverted, so that the sequence of frequency ranges that resulted was, once again nominally, 0 - 10 kHz, 20 - 10 kHz, and 20 - 30 kHz. Taking the lower frequency limit of ~ 400 Hz for the wide-band recording range into account, the actual frequency ranges recorded were ~400 Hz to 10 kHz, ~19.6 to 10 kHz, and ~20.4 to 30 kHz. Thus, as a result of the ~400 Hz lower frequency limit on the recorded data, there is a gap of about 800 Hz, centered on 20 kHz, in the frequency coverage.

The three different wide-band frequency ranges were not recorded for equal lengths of time. Twice as much time (25.6 s) was given to the recording of the lowest frequency range as was given to the intermediate range (12.8 s) or the upper frequency range (12.8 s). The three ranges were recorded sequentially, with the result that a distinctive 2:1:1 pattern emerges in spectrograms of the data. It is important to note that the data in the two frequency ranges not being recorded at any particular time were lost.

The switching between antennas and between the three wide-band frequency ranges was coordinated, with the start of each new interval of recording with a particular antenna (electric, magnetic, or Langmuir probe) also corresponding to the start of one of the 2:1:1 wide-band recording sequences described above. As a result, the two switching patterns do not drift relative to each other. This has the advantage that all combinations of antenna responses and frequency ranges are ultimately covered by the measurements.

Finally, with regard to the ELF data (~5 Hz to 1 kHz) that were also recorded by the wide-band receiver, there is of course only the one fixed frequency range and spectrograms of the recorded data only display the antenna switching pattern. Furthermore, the ELF data were recorded simultaneously with the wide-band data and thus they are continuously available for comparison with the wide-band data in whichever one of the three frequency ranges is effective at the time.

Both the wide-band channel and the ELF channel have automatic gain control (AGC), which functions independently for each channel. It has a 100 db range and it responds to the overall total rms voltage associated with the channel passband. Within the limits of its range and time constant (0.1 - 0.2 s) it keeps the overall voltage out of the passband constant.

Accurate timing is provided by an IRIG-coded time signal that was recorded simultaneously on the wide-band magnetic tape along with the electric and magnetic field data.

3.2 Results

Many hours of magnetic tape data from the wide-band receiver on STS-3 were spectral analyzed and the resulting dynamic spectrograms recorded on film. These films were then examined to see what phenomena occurred in the frequency range 5 Hz - 30 kHz during operation of the FPEG. In addition, the films were also examined at times when the FPEG was not operating, to determine the form of the normal (*i.e.*, non-FPEG) background of electromagnetic noise. It should be stressed that this background is not the normal *natural* background. We have already discussed how the motion of the orbiter can give greatly differing plasma conditions (ram and wake conditions) in the payload bay, where most of our PDP measurements were made, depending on the orientation of the orbiter relative to its direction of motion. It is also likely that the orbiter motion can influence the electromagnetic noise background through, for example, the generation of ion acoustic waves in its turbulent wake [*Shawhan and Murphy 1983*]. There is, in any event, a broadband electromagnetic noise in the range 30 Hz to 100 kHz that appears to be generated by the orbiter's motion through the ambient ionospheric plasma [*Shawhan et al.*, 1984b]. The orbiter is also a very strong source of primarily magnetic noise at discrete frequencies due to the use of various power converters and data clocks both on the orbiter itself and in the payload systems. This electromagnetic interference (EMI) background is of considerable interest because of its implications for future electromagnetic measurements on the orbiter (particularly highly sensitive measurements), and it is discussed in some detail by *Shawhan and Murphy* [1983] and *Shawhan et al.* [1984b].

Despite the presence of the broad band of unstructured electromagnetic noise generated by the orbiter's motion which was most evident in the dynamic spectrograms of electric antenna data, and the many EMI lines, which were mostly only evident in the dynamic

spectrograms of magnetic antenna data (where they largely dominated the spectral data), the measurements made by the electric and magnetic field sensors on the PDP and recorded on the wide-band receiver were often sensitive enough for naturally-occurring ELF and VLF activity (including some strong VLF whistlers) to be clearly evident on the spectrograms, and the signals from ground-based VLF stations, particularly the Omega (U.S.) and Alpha (U.S.S.R.) navigation stations, could also be clearly seen much of the time. More important, from the point of view of the subject of this report, the measurements were sensitive enough for the spectrograms to register the emissions of an electron beam from the FPEG, and during many of the electron beam experiments the spectrograms showed some remarkable electromagnetic effects.

Before describing these specific electromagnetic effects, a comment on the typical 'signature' of an electron beam pulse on the wide-band spectrograms may be of interest. In many cases, when an electron beam is emitted from the FPEG without modulation, there is an immediate change in the gain of the display, even though there is usually no obvious change in the spectral nature of the display. These changes are most obvious in the electric antenna data, which appear to be less affected by the shuttle's EMI, and they take the form of a reduction in gain. In other words, it appears that the unmodulated electron beam produces broad band ELF/VLF electromagnetic noise of sufficient amplitude to produce an AGC response in the wide-band receiver. Once initiated, these changes in gain tend to persist until the electron beam is switched off. Some of these changes in the spectral data are evident in the following display, where we describe one of the unusual effects observed during some of the dc beam sequences.

3.2.1 Results for the DC Beams

In many of the dc beam sequences that we have examined there are no obvious changes in the associated spectrograms of the wide-band data except for the changes in gain corresponding to enhancements of the broad-band electromagnetic noise background that were described above. However, on occasion there appear to be discrete tones generated in the upper part of the ELF frequency range. Furthermore, these tones are primarily magnetic; they can be detected in the electric field data, but they are comparatively very weak.

An example of this tone generation is shown in Figure 2. The dc beam sequences illustrated in the figure started at 0116:48 UT on March 25, 1982 (day 84) and continued for roughly half an hour, with each dc pulse lasting for 53.7 s, as described in Section
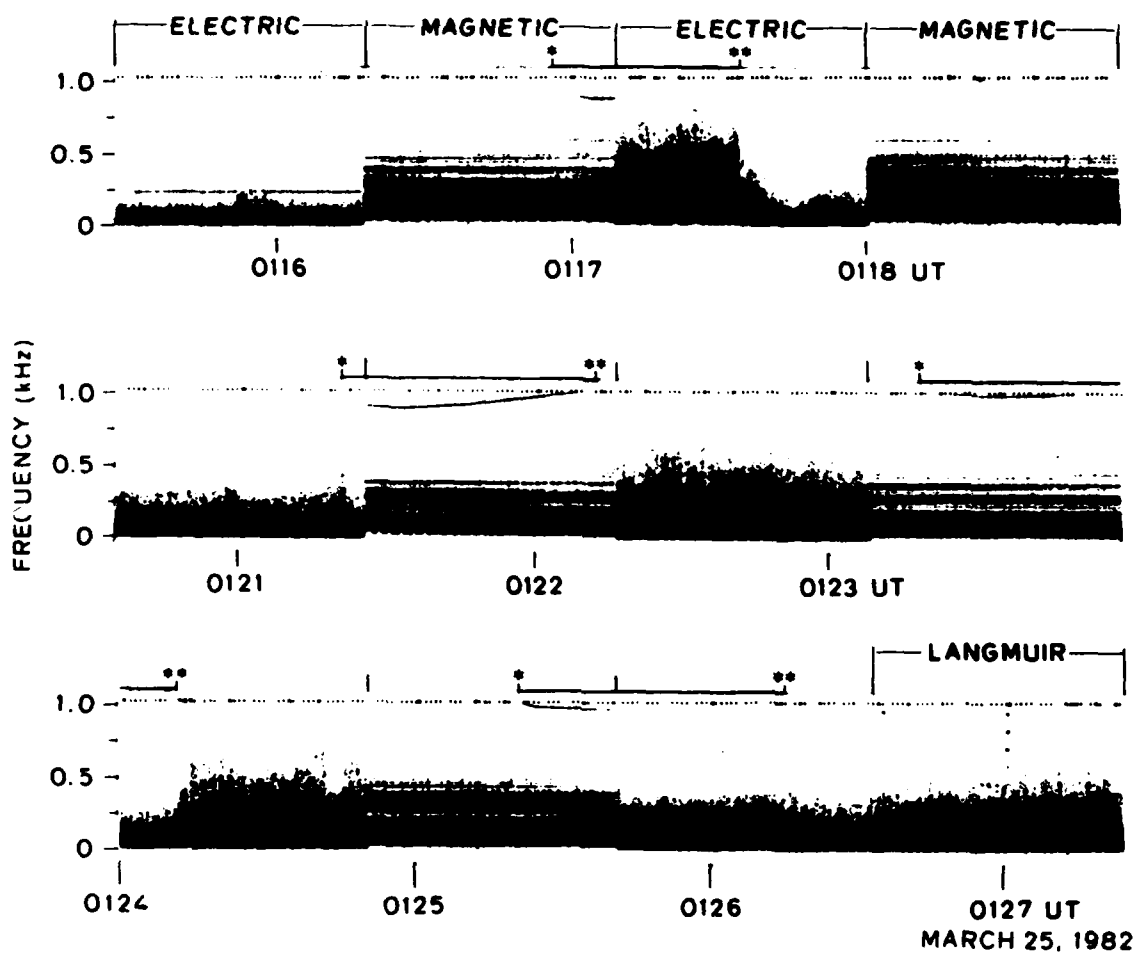
14

Figure 2: Example of dc electron beam pulses generating discrete tones in the upper part of the ELF range. The tones can be seen in the display at frequencies above 800 Hz and following after the start of electron beam emission from the FPEG (indicated by an asterisk in the display). FPEG "off" is denoted by a double asterisk.

2.1. Orbital darkness pertained throughout the experiment. The ELF tones, which have a U-shaped profile in the spectrograms, can be seen toward the top of the display; their frequencies are all close to 1 kHz.

3.2.2 Results for the ULF/ELF Beam Modulations: 1. CC Sequences

In most examples of CC sequence FPEG firings that we have examined there are no obvious changes in the corresponding ELF or wide-band spectrograms other than the changes in gain discussed above. However, in some cases there is evidence for the excitation of a narrow noise band at around 3.5 kHz. An example of this kind of effect is shown in Figure 3.

The PDP was on the pallet in the payload bay while it was making the measurements shown in Figure 3, which apply to the CC sequence starting at 0208:14 UT on day 85. Daylight and wake conditions applied throughout the sequence [*Hawkins*, 1984].

Another similar but more extreme example of band structure associated with the last few sets of pulses in a CC sequence is shown in Figure 4. Once again it is electric field measurements that are shown, but obtained this time with the Langmuir probe. One characteristic of the wide-band receiver measurements made by this latter instrument should be ignored: the probe is subject to a voltage sweep of 1.07 s duration every 12.83 s, which enables the probe to fulfill its primary function of providing a measurement of electron temperature and density but which also produces extraneous 1-second gaps (containing some horizontal spectral lines) in the spectrograms. Two of these sweeps can be seen in the top panel of Figure 4.

The CC sequence shown in Figure 4 was initiated at 0508:23 UT on day 85 and daylight and wake conditions applied throughout the sequence [*Hawkins*, 1984], as was the case for our other example (Figure 3). No beam-related effects are observed for the first nine sets of pulses, apart from the gain changes already discussed, but starting with the 10th set the background noise band, which is centered very roughly on 4 kHz, appears to become entrained. The entrainment is particularly evident during the 11th and 12th sets, and its occurrence is accentuated by the partial recovery that takes place between the two sets (there is also a recovery after the 10th set).

We tentatively ascribe the stimulation of the noise band in Figure 3, and possibly also the noise band during the last two sets of pulses in Figure 4, to the onset of strong beam-plasma interaction, which is only initiated when the electron beam pulse length exceeds
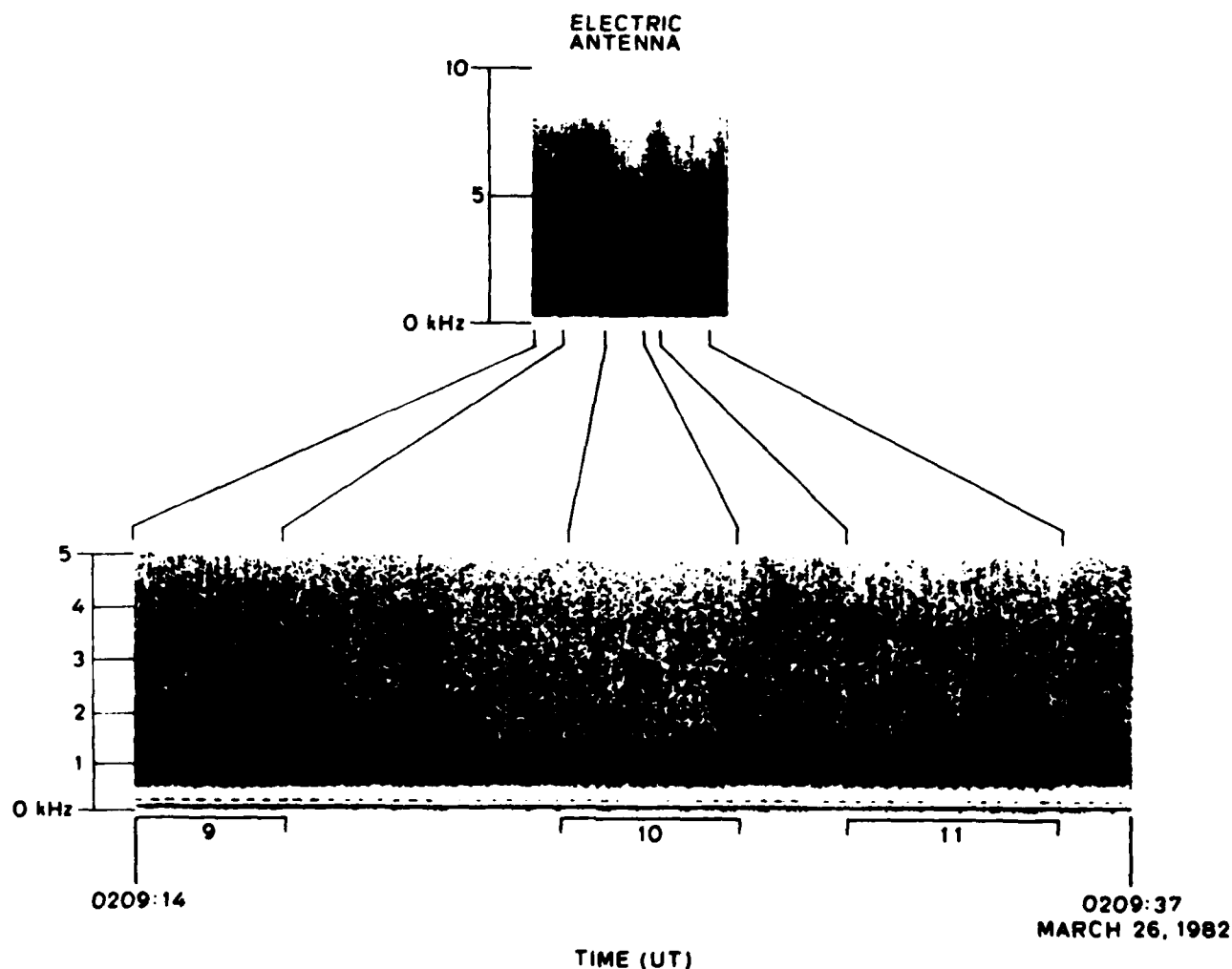
16

Figure 3: Example of noise bands observed during an FPEG CC sequence. This particular sequence was initiated at 0208:14 UT on March 26, 1982 (day 85), and the display covers the 9th, 10th, and 11th of the 12 sets of 16 pulses (the sets are labelled at the bottom of the display). No noise bands are evident in the first nine sets of pulses, but in the 10th and 11th sets an enhancement is evident at about 3.5 kHz. There w.s a change of frequency scale just after the first pulse of the 12th set, which is omitted from the display; however, in the original record a noise enhancement can be seen at around 3.5 kHz at the time of the pulse. Note the changes in gain (most evident in the top panel) during the intervals when the FPEG is emitting pulses.

17

13.11 ms (the on-time for the 9th set of pulses in the CC sequence). If this is the case, we would expect the center frequency of the noise bands to correspond with the local lower hybrid resonance (LHR) frequency. An exact correspondence between the center frequencies in Figures 3 and 4 with the local LHR frequency needs to be established by further research, but we note that the LHR frequency is typically on the order of 5 kHz or less for the plasma conditions pertaining along the STS-3 orbit.

3.2.3 Results for the ULF/ELF Beam Modulations: 2. WS Sequences

Only a limited number of spectrograms of the wide-band and ELF electromagnetic field measurements obtained during the FPEG WS sequences have been examined to date. Nevertheless, it is evident that there are unusual features in the spectrograms of the ELF-range (5 Hz to 1 kHz) data. There do not appear to be any exceptional features in spectrograms of the wide-band data (~400 Hz to 30 kHz); in particular, there are no kilohertz-frequency noise bands similar to those that are observed in some of the CC sequence spectrograms. However, this latter conclusion is subject to change as we analyze further spectrograms of the WS data.

The unusual features we have observed involve the harmonic structure of the signals at moderately low ELF frequencies, i.e., at frequencies less than a few hundred Hz. Figure 5 shows one example of these features. The WS sequence displayed was initiated at 0218:56 UT on March 26, 1982 (day 85); it followed immediately after the CC sequence illustrated in Figure 3 and daylight wake conditions still pertained in the payload bay, although the shuttle would shortly enter the Earth's shadow [Hawkins, 1984]. The spectrogram shown only covers the frequency range ~20 - 100 Hz and the unusual feature is the comparative weakness of the line corresponding to the electron beam modulation at 74.0 Hz. The only explanation we have for this degradation of the 74.0 Hz fields produced by the electron beam is a possible correspondence of the modulation frequency with an ion gyrofrequency. This possibility will be investigated further as more spectrograms of WS sequence data are examined.

The other exceptional feature that is observed in spectrograms of the WS sequence wave data is an apparent displacement in frequency of some of the harmonics associated with the lower frequency modulations of the electron beam. We suspect an instrumental cause for these frequency shifts at the present time, even though there is no evidence for such a cause in the data we have examined so far. Possible small shifts in frequency would not be unexpected, due to the use of analog recording in the wide-band data
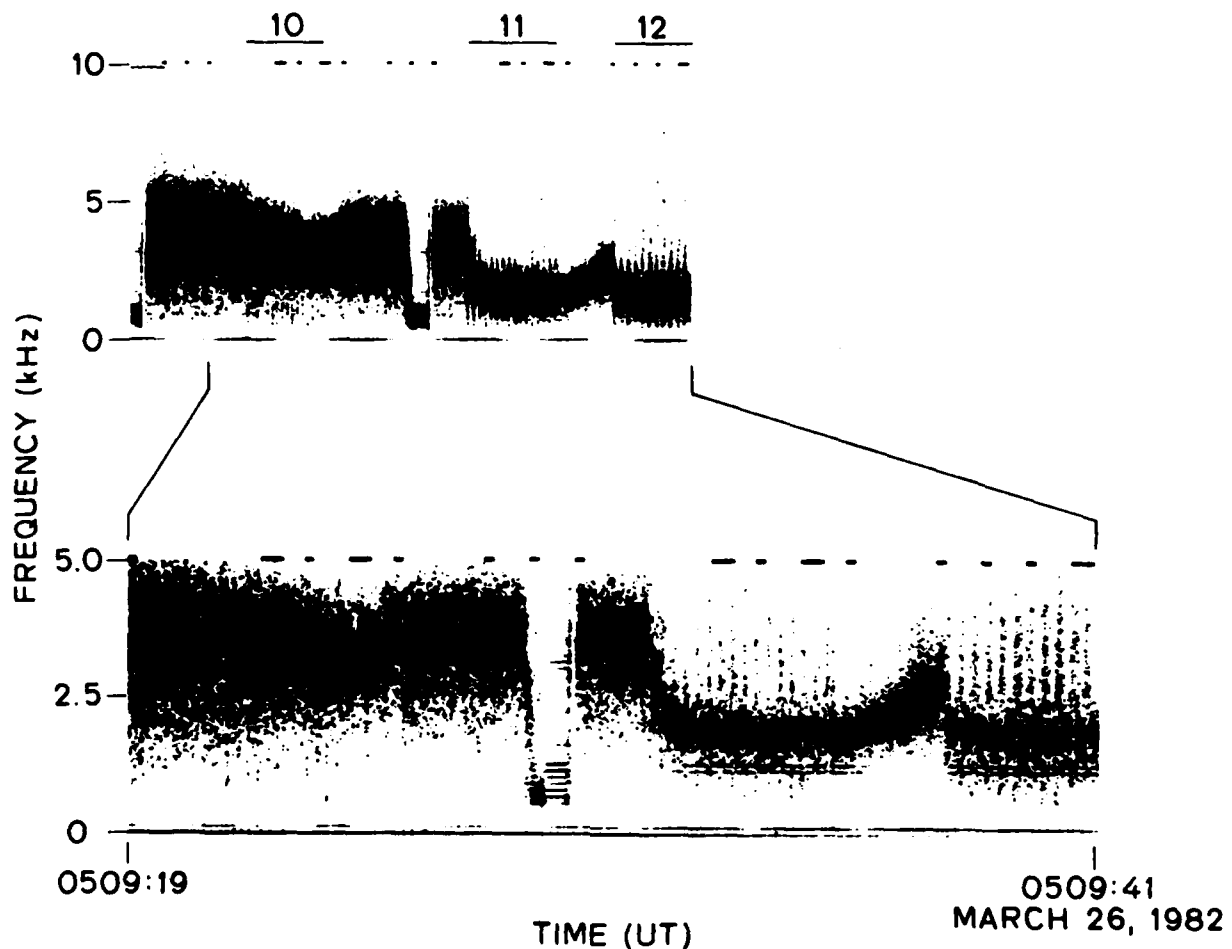
Figure 4: A further example of noise bands observed during an FPEG CC sequence. The sequence was started at 0508:23 UT on March 26, 1982 (day 85), and the display covers the last three of the 12 sets of 16 pulses. The PDP Langmuir probe was used to obtain the electric field measurements. No FPEG-related noise bands are evident in the the first 9 of the sets of pulses, and none are evident here in the 10th set. However, in this latter set there is a change in the background noise during the pulsing and in the 11th and 12th sets the effect is accentuated.

19
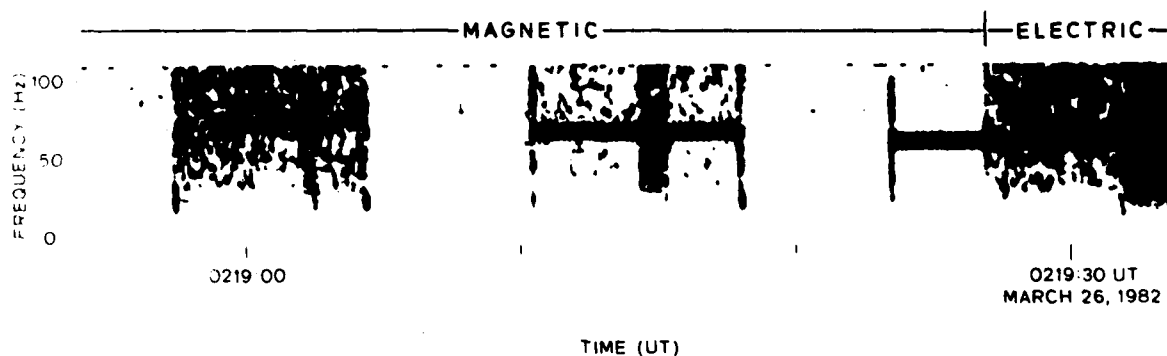
Figure 5: Example of a spectrogram of a WS sequence with a weak frequency component. The first three intervals of modulation of the WS sequence are shown: 74.0 Hz (left), 67.8 Hz (middle), and 61.0 Hz (right), and the unusual feature is the weak spectral component corresponding to the 71.0 Hz modulation of the electron beam - the initial modulation; the lines corresponding to the 67.8 Hz and 61.0 Hz modulations of the beam are comparatively very strong.

20

acquisition system, and these small shifts could assume major proportions when the characteristics of signals with frequencies less than about 20 Hz were being measured. On the other hand, the well-established WS sequence modulation frequencies and their harmonics provide a very effective calibration of the frequency scale, thus helping to eliminate some of the usual uncertainties associated with analog recording. The displacement of harmonics is currently under study.

3.2.4 Results for the VLF Beam Modulations

The VLF electron beam modulation experiments always produce well-defined harmonic patterns on spectrograms of the wide-band electric and magnetic field data. Initially these patterns appeared to be entirely straightforward and they raised few questions. However, when examined carefully, it soon became clear that the harmonic patterns contained a number of anomalous features. At this stage of our analysis it is still possible that some of these features are instrumental, although we have no evidence to suggest that such is the case and most of the anomalous features have properties suggesting interactions between the VLF-modulated electron beams and the ambient plasma.

Figure 6 shows a typical harmonic pattern for the VLF experiment. The data were recorded, using the electric field antenna, during the one-minute interval 2014 - 2015 UT on March 24, 1982 (day 83), while orbital daylight and ram conditions pertained in the payload bay. One interval of 3.251 kHz modulation followed by one of 4.873 kHz is shown on the left hand side of the display and the various possible harmonics are indicated on the right. The spectrogram is a composite, combining a 0 - 10 kHz section at the bottom with an inverted 20 - 10 kHz section on top. Two sets of harmonics are missing in the spectrogram: the harmonics at 9.75 kHz and at 19.51/19.49 kHz. The loss of the harmonics near 20 kHz is expected, because of the recording gap centered on 20 kHz described previously in this report. However, the absence of the 9.75 kHz harmonics is more significant, since the recording system has good sensitivity close to 10 kHz, even though that is the upper limit to the recording range.

To interpret the harmonic structure shown in Figure 6, we apply a basic Fourier series approach, such as is used in the theory of *Harker and Banks* [1984, 1985] for the radiation from modulated electron beams based on coherent spontaneous emission. According to the *Harker and Banks* [1984 1985] theory, the VCAP pulsed electron beam should radiate a series of harmonics, with the electromagnetic power in each
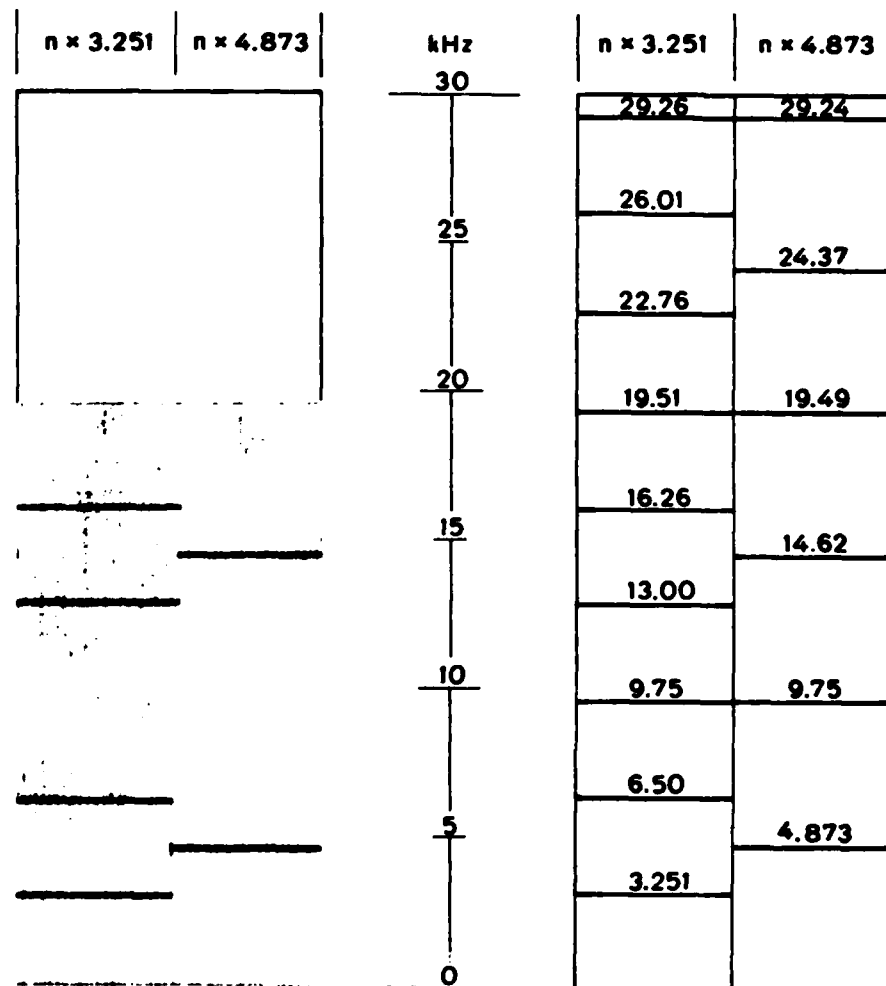
Figure 6: Typical VLF harmonics for the VLF beam modulation experiments. Each harmonic line is well-defined and there are no extraneous lines or noise bands. The only feature of this display that can not be considered typical is the absence of the harmonic lines at 9.75 kHz.

harmonic being proportional to $\sin^2(\pi\gamma d)$, where γ is the harmonic number and d is the pulse duty cycle (i.e., d is the ratio of the pulse on-time to the pulsing period). For the 3.251 kHz modulation of the electron beam, the duty cycle is 2/3 and harmonics corresponding to $\gamma = 3, 6, 9, \ldots$ should not be present. Thus lines should appear in spectrograms of the radiated power only at frequencies of 3.251 kHz, 6.502 kHz, 13.004 kHz, 16.256 kHz, 22.757 kHz, etc. For the 4.873 kHz modulation, the duty cycle is 1/2 and all the even harmonics ($\gamma = 2, 4, \ldots$) should disappear. The corresponding harmonic sequence is 4.873 kHz, 14.619 kHz, 24.365 kHz, etc. It can be seen that the 9.751 kHz and 9.748 kHz harmonics are missing in both series, as is observed in Figure 6.

Figure 7, prepared in the same way as Figure 6, shows the most common anomalous effect we have observed in the VLF-modulation spectrograms. The data were recorded on March 24, 1982 (day 83), during the interval 1709:30 - 1710 UT, using the electric field antenna. Daylight and ram conditions pertained in the payload bay. At the higher frequencies (10 - 30 kHz) there is an extra line just above the normal harmonic lines. The difference in frequency between the extra line and the underlying harmonic line is about 350 Hz and it's always the same, no matter which harmonic or which pulsing frequency is considered. It may also be noticed in Figure 7 that the extra lines tend to become stronger at higher frequencies. This is another persistent characteristic of the extra lines. The display in Figure 7 is interesting for another reason: the harmonics at 9.75 kHz are present.

Finally, in Figure 8 we illustrate two other anomalous features that appear in some of the spectrograms for the VLF beam modulation experiments. In the top panel we show VLF sequence data obtained during the interval 1607 - 1609 UT on March 26, 1982 (day 85), when the payload bay was in darkness and the local plasma and neutral gas were in transition from ram to wake conditions. Conspicuously present in the 3.251 kHz modulation segments of the spectrogram (0 - 10 kHz range) are extra lines at frequencies half way between the normal harmonic lines. We call them 'lines,' but careful inspection of the spectrogram will reveal that some of them more closely resemble narrow noise bands. Furthermore, it will be seen that their amplitudes do not remain constant but decline with time so that the lines have essentially disappeared toward the end of their modulation segments. No extra lines appear half way between the harmonics in the corresponding 4.873 kHz segments of the spectrogram, but it will be seen that an extra line similar to those in the 3.251 kHz modulation segments appears roughly 1.2 kHz above the 4.873 kHz fundamental line in the electric antenna data. Unlike the extra

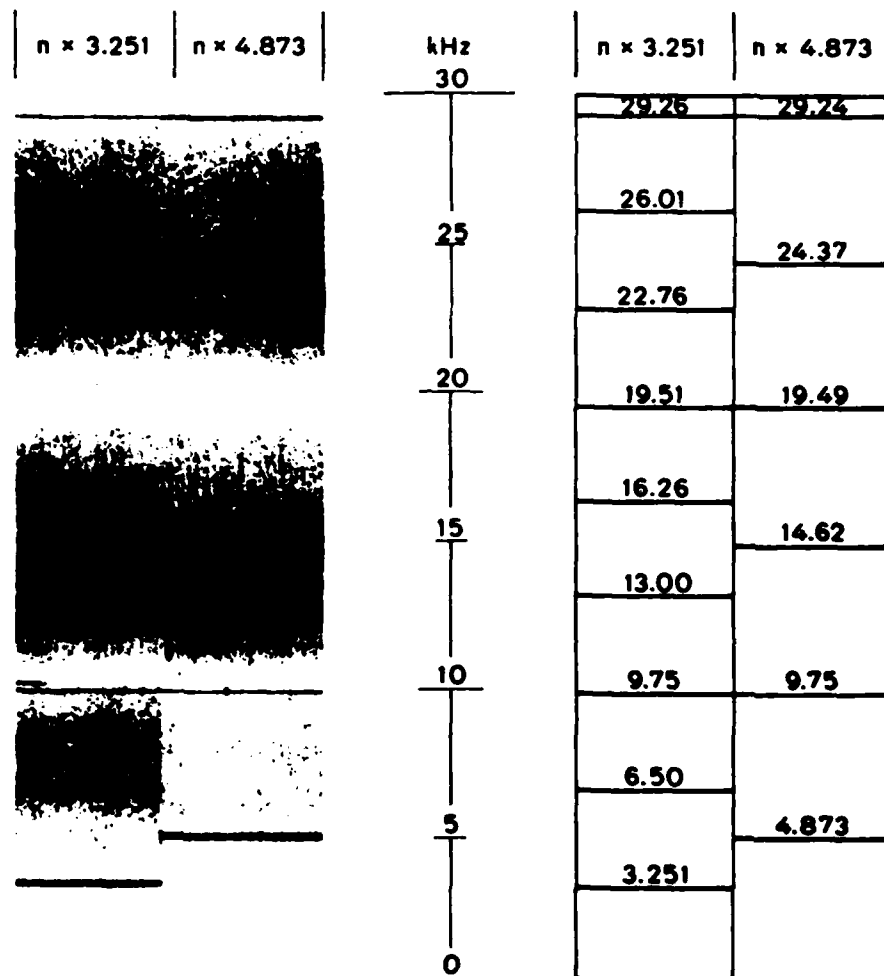| n × 3.251	n × 4.873		kHz	n × 3.251	n × 4.873
			30	29.26	29.24
				26.01	
			25		24.37
				22.76	
			20	19.51	19.49
				16.26	
			15		14.62
				13.00	
			10	9.75	9.75
				6.50	
			5		4.873
				3.251	
			0		

Figure 7: A VLF modulation experiment in which an extra line appears just above the expected harmonic lines.
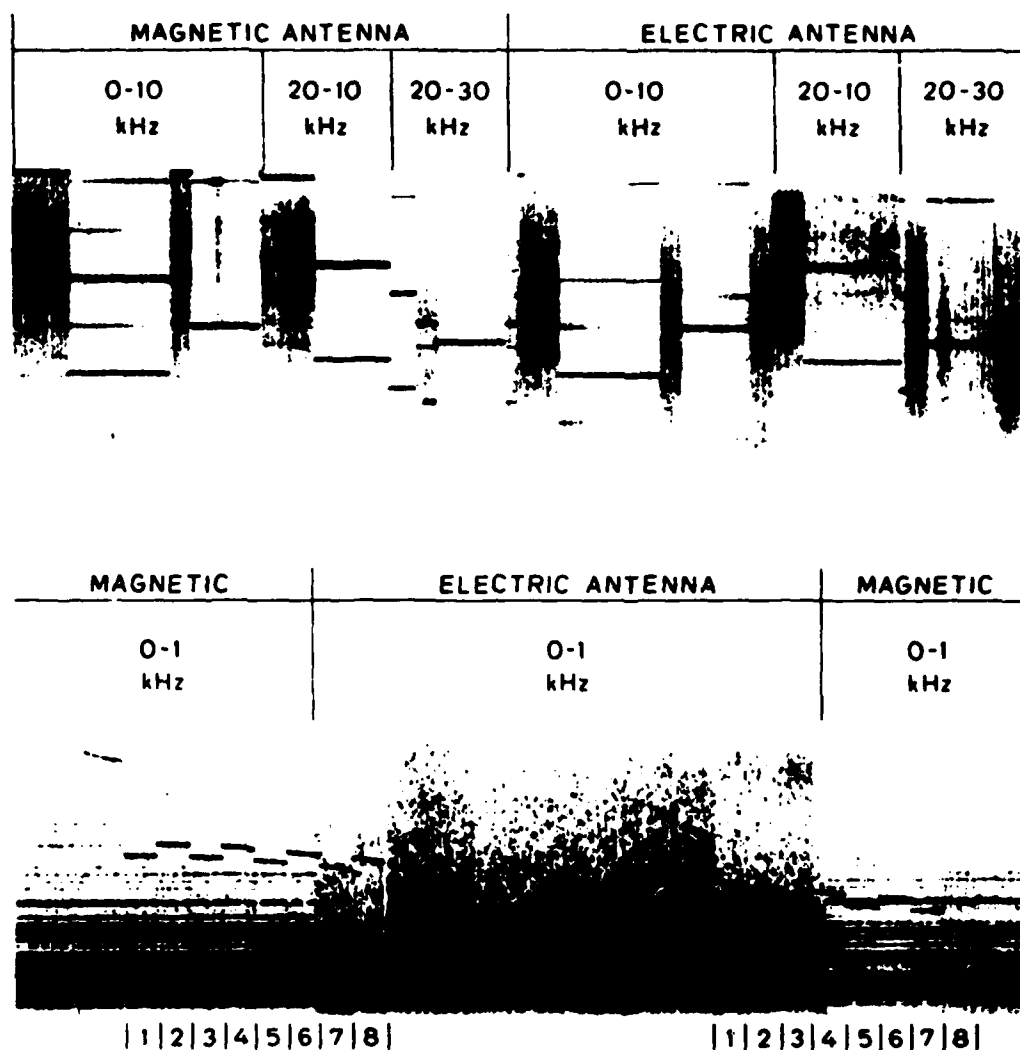
Figure 8: Further anomalous effects observed during the VLF beam modulation experiments. In the top panel, which displays a spectrogram of VLF wide-band data recorded during the interval 1607 - 1609 UT on March 26, 1982 (day 85), a number of even harmonic lines (or narrow noise bands) can be seen occurring in conjunction with the normal odd harmonic lines. Two examples of lines at half the fundamental 3.251 kHz frequency can also be seen, and, in one instance, a 'line' appears roughly 1.2 kHz above one of the 4.873 kHz lines. Signals from the Soviet Alpha navigation station at Komsomolskamur can be seen in the initial half of the magnetic antenna record for the frequency range 20 - 10 kHz (the line at roughly 11.6 kHz is orbiter EMI). The bottom panel shows some unexpected signals that are observed in the ELF range during the VLF modulation experiment that took place from 2226 - 2228 UT on March 24, 1982 (day 83).

lines in the 3.251 kHz segments, the amplitude of this latter line increases with time. Two examples of other additional lines can also be seen in the spectrogram. They appear below the 3.251 kHz fundamental lines (at half the fundamental frequency) in both the electric and magnetic antenna data. Interestingly, the 9.75 kHz harmonics are present, and their amplitudes increase with time in the frequency segments that are displayed.

Recent computations we have made indicate that the electron beam did not depart cleanly from the orbiter during this VLF sequence; instead, its helical path intercepted one of the orbiter's surfaces. It would be easy to ascribe the unusual lines in the spectrogram to this circumstance. However, the spectral data shown in Figure 6, which appear to be typical in every way, were also obtained for an intercepted beam.

The bottom panel of Figure 8 shows a peculiar manifestation of the VLF modulation that appears in the ELF range. The data were recorded, using both electric and magnetic antennas as indicated in the figure, during the interval 2226 - 2228 UT on March 24, 1982 (day 83). Orbital darkness and wake conditions applied in the payload bay and, once again, it is probable that the electron beam was intercepted by one of the orbiter's surfaces. The roughly square modulation of the signals appearing in the spectrogram coincides with the switching between 3.251 kHz and 4.873 kHz in the VLF modulation sequence. This ELF signal could be interpreted as being the result of an instrumental effect (perhaps a form of intermodulation) were it not for the steady decline in frequency of the signals.

4. DISCUSSION

This preliminary study of the wide-band electric and magnetic field data recorded during the modulated electron beam experiments on STS-3 has revealed a number of anomalous effects that may well involve some forms of beam-plasma interactions. These effects may be enumerated as follows:

1. ELF/VLF bands excited during ULF pulsed operation of the electron beam.

2. Generation of side frequencies, additional harmonic lines, and other extra spectral lines during VLF pulsed operation of the electron beam.

3. Generation of discrete tones during dc pulsed operation of the electron beam.

4. Peculiarities in the lower-ELF harmonic structure produced during lower-ELF pulsed operation of the electron beam.

Studies of these various effects are continuing. The results will have important implications for the use of modulated electron beams in space as wireless antennas for the generation of low frequency signals.

5. REFERENCES

Banks, P.M., W.J. Raitt, P.R. Williamson, A.B. White, and R.I. Bush, Results from the vehicle charging and potential experiment on STS-3, to appear in *AIAA J. Spacecraft Rockets*, 1985.

Cambou, F., J. Lavergnat, V.V. Migulin, A.I. Morozov, B.E. Paton, R. Pellat, A.Kh. Pyatsi, H. Reme, R.Z. Sagdeev, W.R. Sheldon, I.A. Zhulin, ARAKS - Controlled or puzzling experiment?, *Nature, 271*, 723, 1978.

Cartwright, D.G., and Kellogg, P.J., Controlled experiments on wave-particle interactions in the ionosphere, *Nature, 231*, 11, 1971.

Cartwright, D.G., and P.J. Kellogg, Observations of radiation from an electron beam artificially injected into the ionosphere, *J. Geophys. Res., 79*, 1439, 1974.

Grandal, B, (Ed.), *Artificial Particle Beams in Space Plasma Studies*, 704 pp., Plenum Press, New York, 1982.

Harker, K.J., and P.M. Banks, Radiation from pulsed electron beams in space plasmas, *Radio Sci., 19*, 454, 1984.

Harker, K.J., and P.M. Banks, Radiation from long pulse train electron beams in space plasmas, to appear in {Planet. Space Sci.}, 1985.

Hawkins, J., Users guide to the STS-3 attitude and trajectory information in VCAP coordinates, Tech. Rept., STAR Laboratory, Stanford University, Stanford, California, September 1984.

Hendrickson, R.A., R.W. McEntire, and J.R. Winckler, Electron Echo experiment: A new magnetospheric probe, *Nature, 230*, 564, 1971.

Hess, W.N., Generation of artificial aurora, *Science, 164*, 1512, 1969.

Linson, L.M., and K. Papadopoulos, Review of the status of theory and experiment for injection of energetic electron beams in space, Tech. Rept. No. SAI-023-80-459-LJ, Science Applications Inc., La Jolla, California, April 1980.

Meltzner, F., G. Metzner, and D. Antrack, The GEOS electron beam experiments S-329, *Space Sci. Instr., 4*, 45, 1978.

Neupert, W.M., P.M. Banks, G.E. Bruekner, E.G. Chipman, J. Cowles, J.A.M. McDonnell, R.Novik, S. Ollendorf, S.D. Shawhan, J.J. Trilio, and J.J. Weinberg, Science on the space shuttle, *Nature, 296*, 193, 1982.

Shawhan, S.D., and G.B. Murphy, Plasma diagnostics package assessment of the STS-3 orbiter environment and systems for science, paper presented at the AIAA 21st Aerospace Sciences Meeting, Reno, Nevada, January 10-13, 1983.

Shawhan, S.D., G.B. Murphy, P.M. Banks, P.R. Williamson, W.J. Raitt, Wave emissions from dc and modulated electron beams on STS-3, *Radio Sci., 19*, 471, 1984a.

Shawhan, S.D., G.B. Murphy, and J.S. Pickett, Plasma diagnostics package initial assessment of the shuttle orbiter plasma environment, *J. Spacecraft Rockets, 21*, 387, 1984b.

Shawhan, S.D., G.B. Murphy, and D.L. Fortna, Measurements of electromagnetic interference on OV102 Columbia using the plasma diagnostics package, *J. Spacecraft Rockets, 21*, 392, 1984c.

Winckler, J.R., J.E. Steffen, P.R. Malcolm, K.N. Erickson, Y. Abe, and R.L. Swanson, Ion resonances and ELF wave production by an electron beam injected into the atmosphere: Echo 6, *J. Geophys. Res., 89*, 7565, 1984.

Winckler, J.R., The application of artificial electron beams to magnetospheric research, *Rev. Geophys. Space Phys., 18*, 659, 1980.

APPENDIX

Plasma Diagnostics Package Instrumentation

1. Langmuir probe. Measures thermal electron densities between 10^4 and 10^7 cm^{-3}, and the spectrum of electron density fluctuations in the frequency range 4 - 60 Hz.

2. Low energy proton and electron differential energy analyzer (LEPEDEA). Measures nonthermal electron and proton energy spectra and pitch angle distributions for particle energies in the range 2 eV - 50 keV.

3. Search coil. Measures the amplitude of magnetic field fluctuations with frequencies in the range 10 Hz - 30 kHz.

4. AC electric field wave analyzer. Measures electric fields with frequencies in the range 10 Hz - 1 GHz.

5. Retarding potential analyzer (RPA) and associated differential ion flux probe (DIFP). Measures the ion number density from 10^2 - 10^7 cm^{-3}. Also measures the energy distribution function below 16 eV and directed ion velocities up to 15 km/s.

6. Ion mass spectrometer. Measures ion masses in the range 1 - 64 atomic mass units, and ion densities in the range 20 to 20 $\times$ 10^7 ions/cm^3.

7. DC electrostatic double probe with spherical sensors. Measures dc electric fields in one axis from 2 mV/m to 2 V/m.

8. DC triaxial fluxgate magnetometer. Measures dc magnetic fields with amplitudes in the range 12 mG to 1.5 G (1.2×10^{-7} to 1.5×10^{-4} T).

9. Total energetic electron fluxmeter. Measures energetic electron fluxes in the range 10^9 - 10^{14} electrons/cm^2.s.

10. Pressure gauge. Measures ambient pressure from 10^{-3} - 10^{-7} torr.

MISSION
of
Rome Air Development Center

RADC plans and executes research, development, test and selected acquisition programs in support of Command, Control Communications and Intelligence (C^3I) activities. Technical and engineering support within areas of technical competence is provided to ESD Program Offices (POs) and other ESD elements. The principal technical mission areas are communications, electromagnetic guidance and control, surveillance of ground and aerospace objects, intelligence data collection and handling, information system technology, solid state sciences, electromagnetics and electronic reliability, maintainability and compatibility.

END

FILMED

1-86

DTIC